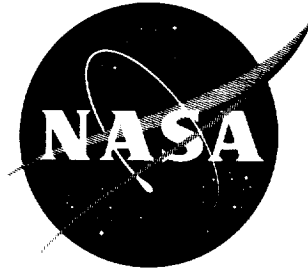


29.



N 68 167-5

Spencer

TECHNICAL NOTE

D-1810

VIBRATIONAL-NONEQUILIBRIUM FLOW OF NITROGEN

IN HYPERSONIC NOZZLES

By Wayne D. Erickson

Langley Research Center
Langley Station, Hampton, Va.

NATIONAL AERONAUTICS AND SPACE ADMINISTRATION
WASHINGTON

June 1963

NATIONAL AERONAUTICS AND SPACE ADMINISTRATION

TECHNICAL NOTE D-1810

VIBRATIONAL-NONEQUILIBRIUM FLOW OF NITROGEN

IN HYPERSONIC NOZZLES

By Wayne D. Erickson

SUMMARY

The various free-stream flow parameters have been calculated for vibrational-nonequilibrium flow of nitrogen in hypersonic nozzles based on a quasi-one-dimensional analysis. The results are presented for stagnation temperatures ranging from 1,000° K to 5,000° K and for a practical range of a single nozzle-characteristic quantity that accounts for stagnation pressure, throat radius, and nozzle expansion angle. It is shown that for some practical nozzle conditions, the vibrational-nonequilibrium effects can significantly influence the free-stream nozzle-flow parameters.

INTRODUCTION

There are a number of hypersonic test facilities presently using nitrogen, rather than air, as the test gas. A large portion of these facilities are used to simulate Mach number and Reynolds number combinations without attempting to study high enthalpy effects. The Hotshot-type tunnel is often operated with nitrogen at stagnation temperatures near 3,000° K and stagnation pressures of about 1,000 atmospheres producing flows with a Mach number of about 20. Hypersonic tunnels powered by a steady electric arc or by an electrical resistance heater have also used nitrogen as the test gas.

The use of nitrogen practically eliminates the heater-component-oxidation problem and still gives experimental data which are essentially the same as one would obtain with air under the same test conditions, as long as the corresponding air temperature is not so great as to cause significant dissociation. A problem, however, which is common to both the air and nitrogen systems, even when the test gas is essentially completely in the molecular state but at moderately high temperatures, is the degree to which molecular vibrational relaxation can affect the nozzle-flow process.

In reference 1 the effects of molecular vibrational relaxation on hypersonic-nozzle flows in air have been examined. The main concern was with the calculation of the difference between the vibrational and translational temperatures of the stream of an expanding flow in a hypersonic nozzle and the measurement of temperature in the test section of an intermittent hypersonic tunnel using the

r^*	nozzle throat radius
T	translational temperature
t	time
v	velocity
v_l	limiting velocity
v_l'	limiting velocity based on $h_o = c_p'T_o$
x	distance from throat along nozzle axis
$\Gamma(\gamma)$	function defined by equation (23)
γ	ratio of heat capacities
γ'	ratio of heat capacities including effects of translational and rotational energy modes only; $7/5$
θ	nozzle half-angle
Θ	molecular vibrational temperature for nitrogen, $^{\circ}\text{K}$
ρ	density
σ	vibrational energy
τ	vibrational-relaxation time, defined by equation (14)
$\psi_T, \psi_p, \psi_\rho, \psi_v, \psi_M, \psi_q$	ratio of free-stream parameters T , p , ρ , v , M , and q calculated for vibrational-nonequilibrium flow divided by that calculated for vibrational-equilibrium flow at the same area ratio and stagnation conditions

Subscripts:

e	equilibrium conditions
f	results for frozen flow, that is, $\gamma = 7/5$
o	nozzle stagnation conditions

Superscript:

$*$	conditions at nozzle throat
-----	-----------------------------

where Θ is the characteristic temperature of molecular vibration and is equal to 3,336.6° K for nitrogen.

In this analysis it is assumed that the gas obeys the ideal-gas equation

$$p = \rho RT \quad (7)$$

The relation between the cross-sectional area of the nozzle at any position and the distance along the nozzle axis from the throat is taken to be

$$\frac{A}{A^*} = 1 + \left(\frac{\tan \theta}{r^*} \right)^2 x^2 \quad (8)$$

where the nozzle becomes conical with half-angle θ at large distances from the throat. Because θ and r^* always appear grouped together as indicated in equation (8), it is convenient to define a single nozzle characteristic that includes these two quantities as was done in the work of reference 5, namely,

$$l = \frac{r^*}{\tan \theta} \quad (9)$$

Equilibrium Flow

The foregoing system of simultaneous equations is sufficient for calculating the various flow properties along the nozzle for equilibrium conditions. The first step in the calculation procedure is to specify the nozzle stagnation conditions T_0 and p_0 . Inasmuch as it is desired to calculate the various nozzle flow properties as a function of nozzle area ratio A/A^* , it is not necessary to specify the nozzle size or shape for the equilibrium flow calculations; that is, equations (8) and (9) are not used for the equilibrium case.

The various isentropic-equilibrium flow equations with vibrational energy effects included have been developed and presented in reference 4. The expression for the free-stream pressure as a function of free-stream temperature and stagnation conditions presented in reference 4 is

$$p = C_0 T^c p'^{1/R} \frac{1}{1 - \exp \frac{\Theta}{T}} \exp \left(\frac{\Theta}{T} \frac{\exp \frac{\Theta}{T}}{\exp \frac{\Theta}{T} - 1} \right) \quad (10)$$

where

$$C_0 = p_0(T_0)^{-c} p'^{1/R} \left(1 - \exp \frac{\Theta}{T_0} \right) \exp \left(- \frac{\Theta}{T_0} \frac{\exp \frac{\Theta}{T_0}}{\exp \frac{\Theta}{T_0} - 1} \right)$$

The free-stream pressure p can, therefore, be determined for a given set of stagnation conditions and a chosen free-stream temperature. The free-stream

Nonequilibrium Flow

The calculation of the flow parameters in a nozzle for the nonequilibrium-flow condition requires a rate expression for the vibrational-relaxation process in addition to the various flow equations and nozzle shape as defined by equation (8). The rate expression for vibrational relaxation is taken to be

$$\frac{d\sigma}{dt} = \frac{\sigma_e - \sigma}{\tau} \quad (14)$$

where τ is the vibrational-relaxation time. In reference 6 is presented a correlation for the vibrational-relaxation time for nitrogen based on an empirical correlation of the data of Blackman as

$$\tau_p = 1.1 \times 10^{-11} T^{1/2} \exp \frac{154}{T^{1/3}} \text{ atm-sec} \quad (15)$$

Now, inasmuch as the local velocity is

$$v = \frac{dx}{dt} \quad (16)$$

t can be eliminated from equation (14) to give

$$\frac{d\sigma}{dx} = \frac{\sigma_e - \sigma}{v\tau} \quad (17)$$

For the nonequilibrium-flow condition it is assumed that the vibrational energy is in equilibrium with the translational and rotational energy modes for the flow process from the nozzle stagnation conditions up to the throat. Downstream of the throat the vibrational energy is allowed to relax at a finite rate according to equation (17) and equation (15). The conditions at the throat are, therefore, calculated from the equilibrium expressions presented in the previous section and serve as the starting point for the nonequilibrium calculations.

The foregoing system of equations which include the vibrational-rate equation can be reduced to a set of two differential equations, each of which contains only the variables T , σ , and x for a given nozzle with a fixed stagnation condition. These two equations are

$$\frac{dT}{dx} = \frac{\frac{2x}{l^2 + x^2} + \left[1 - \frac{RT}{2(h_0 - c_p'T - \sigma)} \right] \frac{\rho^* v^* (\sigma_e - \sigma)}{2\tau p (h_0 - c_p'T - \sigma) (1 + x^2/l^2)}}{\frac{c_p'}{2(h_0 - c_p'T - \sigma)} - \frac{c_p' - R}{RT}} \quad (18)$$

RESULTS AND DISCUSSION

Calculated Results

Numerical results have been obtained for both quasi-one-dimensional non-equilibrium flow and equilibrium flow of molecular nitrogen in hypersonic nozzles having a hyperbolic shape described by equation (8). A number of nozzle-flow parameters were calculated as a function of nozzle area ratio for a range of nozzle stagnation conditions and nozzle characteristics.

The effect of the finite rate of vibrational adjustment on the distribution of the vibrational energy σ along a typical nozzle is shown in figure 1. The ratio of the vibrational energy at any nozzle location to the vibrational energy in the stagnation chamber σ/σ_0 is plotted against the nozzle area ratio for a stagnation temperature of $3,000^\circ$ K. The results for vibrational equilibrium are also shown for comparison. It has already been shown that the nozzle half-angle θ and the nozzle throat radius r^* enter into the nonequilibrium calculations in such a way that both of these nozzle parameters can be combined into a single correlating parameter l defined by equation (9). During the course of these calculations it was also found that the product of the nozzle characteristic l and the stagnation pressure p_0 is a single correlating group. The nonequilibrium results presented in figure 1 were calculated for values of the parameter $p_0 \times l$ equal to 10 , 10^2 , 10^3 , and 10^4 atm-cm, which represent reasonable combinations of stagnation pressures and nozzle shapes and sizes.

Figure 1 shows that the vibrational energy decreases rapidly and steadily with area ratio for the equilibrium-flow case, and it is independent of the quantity $p_0 \times l$. On the other hand, the nonequilibrium calculations depend rather strongly on the quantity $p_0 \times l$. The greater the stagnation pressure p_0 or the nozzle characteristic l , the smaller the departure from equilibrium. The effect of increasing pressure is to increase the rate of vibrational adjustment, and the larger values of l correspond to smaller rates of flow expansion. Each of these effects tends to drive the solution towards the equilibrium result.

Similar calculations have been made for stagnation temperatures from $1,000^\circ$ K to $5,000^\circ$ K in intervals of $1,000^\circ$ K and for the same range of the quantity $p_0 \times l$. These calculations include the nozzle parameters T , p , ρ , v , M , and q for the equilibrium flow as well as for nonequilibrium flow. In order to facilitate the presentation of these results, the nozzle-flow parameters based on nonequilibrium calculations were divided by the corresponding parameters based on vibrational equilibrium for the same stagnation condition and area ratio. These results are presented in figures 2 to 7. Figure 2 shows the ratio of the free-stream (translational) temperature based on nonequilibrium flow divided by the temperature based on equilibrium flow ψ_T . It can be seen from this figure that the quantity ψ_T is essentially independent of area ratio for the range of conditions considered. The complete lack of vibrational-nonequilibrium effects would be indicated by ψ_T equal to unity. The smaller

facilitated by measuring the total pressure behind a normal shock p_o' with a pitot-survey probe. Calculation of the conditions behind normal shocks have not been carried out in this present work, but a simple approximate method for relating p_o' to the free-stream parameters is presented here.

The ratio of the free-stream dynamic pressure to the stagnation pressure of the nozzle for flow with γ equal to a constant as given in reference 8 is

$$\frac{q}{p_o} = \frac{\gamma}{2} M^2 \left(1 + \frac{\gamma-1}{2} M^2 \right)^{-\frac{\gamma}{\gamma-1}} \quad (20)$$

Also from reference 8, the ratio of the total pressure behind a normal shock to the stagnation pressure of the nozzle for flow with γ equal to a constant is

$$\frac{p_o'}{p_o} = \left[\frac{(\gamma+1)M^2}{(\gamma-1)M^2 + 2} \right]^{\frac{\gamma}{\gamma-1}} \left[\frac{\gamma-1}{2\gamma M^2 - (\gamma-1)} \right]^{\frac{1}{\gamma-1}} \quad (21)$$

Equation (20) is now divided by equation (21) and, with some rearrangement, the following equation results:

$$\frac{q}{p_o'} = \left(\frac{4}{\gamma} \right)^{\frac{1}{\gamma-1}} \left(\frac{\gamma}{\gamma+1} \right)^{\frac{\gamma+1}{\gamma-1}} \left[1 - \left(\frac{\gamma-1}{2\gamma} \right) \frac{1}{M^2} \right]^{\frac{1}{\gamma-1}} \quad (22)$$

If attention is limited to high Mach numbers, so that $M^2 \gg 1$, and because γ must be in the restricted range $9/7 < \gamma < 7/5$ the last term on the right-hand side of this equation is essentially unity. This term is approximately 0.996 for $M = 10$ and $9/7 < \gamma < 7/5$. At higher Mach numbers this term is even closer to unity and is, therefore, taken to be unity. The remaining terms on the right-hand side of this equation are functions of γ only and the quantity $\Gamma(\gamma)$ is defined as

$$\Gamma(\gamma) \equiv \left(\frac{4}{\gamma} \right)^{\frac{1}{\gamma-1}} \left(\frac{\gamma}{\gamma+1} \right)^{\frac{\gamma+1}{\gamma-1}} \quad (23)$$

so that approximately, but quite accurately,

$$\frac{q}{p_o'} = \Gamma(\gamma) \quad (24)$$

for $M^2 \gg 1$.

The parameter $\Gamma(\gamma)$ is plotted against γ in figure 9 for values of γ of interest in this work. It is seen from this figure that $\Gamma(\gamma)$ is a very weak function of γ and could be taken to be a constant equal to 0.5384 ± 0.85 per cent for the range $9/7 < \gamma < 7/5$.

M is large, as is shown later. The flow ratio q/p_0 for this example is, therefore, 0.5394×10^{-3} .

With this value of q/p_0 and with the use of the tables presented in reference 8, which are based on a constant value of $\gamma = 7/5$, a rough estimate of the area ratio is found, namely, $A/A^* \approx 1,650$. For $T_0 = 3,000^\circ \text{K}$ and the quantity $p_0 \times l = 100 \text{ atm-cm}$, it is determined from figure 7 that $\psi_{q,f} = 0.830$ and $\psi_q = 0.965$. Because $\psi_{q,f}$ and ψ_q are weak functions of area ratio, only a very approximate value of A/A^* was required in order to use figure 7. The ratio of these two quantities $\psi_{q,f}/\psi_q$ represents the ratio of the parameter q based on the assumption of frozen flow with $\gamma = 7/5$ to that based on vibrational-nonequilibrium flow with $T_0 = 3,000^\circ \text{K}$, $p_0 \times l = 100 \text{ atm-cm}$, and $A/A^* \approx 1,650$. The exact value of A/A^* can now be determined by multiplying the ratio $\psi_{q,f}/\psi_q$ by the quantity q/p_0 to find the corresponding frozen-flow value of q/p_0 based on $\gamma = 7/5$; that is,

$$\left(\frac{q}{p_0}\right)_f = \frac{0.830}{0.965}(0.539 \times 10^{-3}) = 0.463 \times 10^{-3}$$

Again from the tabulated flow parameters for $\gamma = 7/5$ presented in reference 8, the value of A/A^* , that corresponds to $(q/p_0)_f = 0.463 \times 10^{-3}$, is equal to 1,929. This is the value for the area ratio for the nonequilibrium-flow case as well as for the frozen-flow case with $\gamma = 7/5$.

The corresponding values of the other free-stream parameters for frozen flow with $\gamma = 7/5$, also determined from reference 8, are:

$$\left(\frac{T}{T_0}\right)_f = 0.2842 \times 10^{-1}$$

$$\left(\frac{p}{p_0}\right)_f = 0.3869 \times 10^{-5}$$

$$\left(\frac{\rho}{\rho_0}\right)_f = 0.1362 \times 10^{-3}$$

$$\left(\frac{v}{a^*}\right)_f = 2.414432$$

$$M_f = 13.07$$

Because a^* is not the same for nonequilibrium flow as it is for frozen flow, it is not convenient to use the quantity $(v/a^*)_f$, but rather $(v/v_l)_f$. It is easily shown that for a flow with γ constant,

$$M = \frac{\psi_M}{\psi_{M,f}} M_f = \frac{1.088}{1.106} 13.07 = 12.85$$

Because the value of the limiting velocity v_l in the ratio $(v/v_l)_f$ differs from that calculated for the case with vibrational equilibrium in the stagnation chamber, the ratio v/v_l for the nonequilibrium case is determined in a similar way, but by multiplying by an additional term $v_l'/v_{l,e}$, which represents the ratio of the limiting velocity based on the exclusion of the vibrational energy term from the stagnation enthalpy to that based on a stagnation enthalpy for vibrational equilibrium. This term is presented in figure 11 as a function of T_0 and was calculated from the equation

$$\frac{v_l'}{v_{l,e}} = \sqrt{\frac{c_p' T_0}{c_p' T_0 + \sigma_{e,o}}} \quad (27)$$

The limiting-velocity ratio for this example is

$$\frac{v}{v_l} = \frac{\psi_v}{\psi_{v,f}} \left(\frac{v}{v_l} \right)_f \frac{v_l'}{v_{l,e}} = \frac{0.965}{0.868} (0.8750)(0.930) = 0.904$$

where $v_l'/v_{l,e}$ is obtained from figure 11 for $T_0 = 3,000^\circ \text{K}$. These are the free-stream flow parameters based on nonequilibrium calculations for this illustrative example.

The charts presented herein may also be used to determine the flow parameters for vibrational-equilibrium flow. This may be done by using the foregoing method, but by setting ψ_q , ψ_T , ψ_p , ψ_ρ , ψ_v , and ψ_M equal to unity. These results, however, do not take into account the real-gas effect due to high densities.

Similar charts have been presented in the work of reference 9 for air for equilibrium flow that do include the real-gas effect due to high densities as well as vibrational energy. In order to obtain an approximate indication of this density effect in nitrogen, one may use the results of reference 9 for air to relate the real-gas equilibrium-flow parameters to those for frozen flow with $\gamma = 7/5$. The various ratios of the flow parameters presented in reference 9, as well as the correction factors presented in reference 8 for vibrational-equilibrium flow of air as an ideal gas, are presented as ratios at fixed Mach numbers rather than at fixed area ratios as in this work. The use of the ratios presented in references 8 and 9 is similar to the procedure presented herein, except it must be remembered that the ratios of the flow parameters for the present work are for the same area ratio.

The real-gas effect due to high densities could be included in the nonequilibrium-flow calculations by using values of $\psi_{q,f}$, $\psi_{T,f}$, $\psi_{p,f}$, $\psi_{\rho,f}$,

CONCLUDING REMARKS

Quasi-one-dimensional calculations of the free-stream flow parameters in hypersonic nozzles for nitrogen with consideration of vibrational-nonequilibrium effects have been carried out. Results have also been obtained for comparison of vibrationally frozen flow and vibrational-equilibrium flow. The calculated results are presented for stagnation temperatures from $1,000^{\circ}$ K to $5,000^{\circ}$ K and indicate that vibrational-nonequilibrium effects can significantly affect the various flow parameters in hypersonic nozzles, particularly at the higher stagnation temperatures where the contribution of the vibrational energy is rather large.

The calculated results are presented in the form of charts which may be used to estimate the vibrational-nonequilibrium effect of nitrogen in a hypersonic nozzle. The nonequilibrium effect is presented as a function of stagnation temperature and for a practical range of a single nozzle characteristic which includes the nozzle size, shape, and stagnation pressure. A useful approximate relation for estimating the free-stream flow quantities for vibrational-nonequilibrium flow from a pitot-pressure measurement in the flow is also included.

Langley Research Center,
National Aeronautics and Space Administration,
Langley Station, Hampton, Va., April 2, 1963.

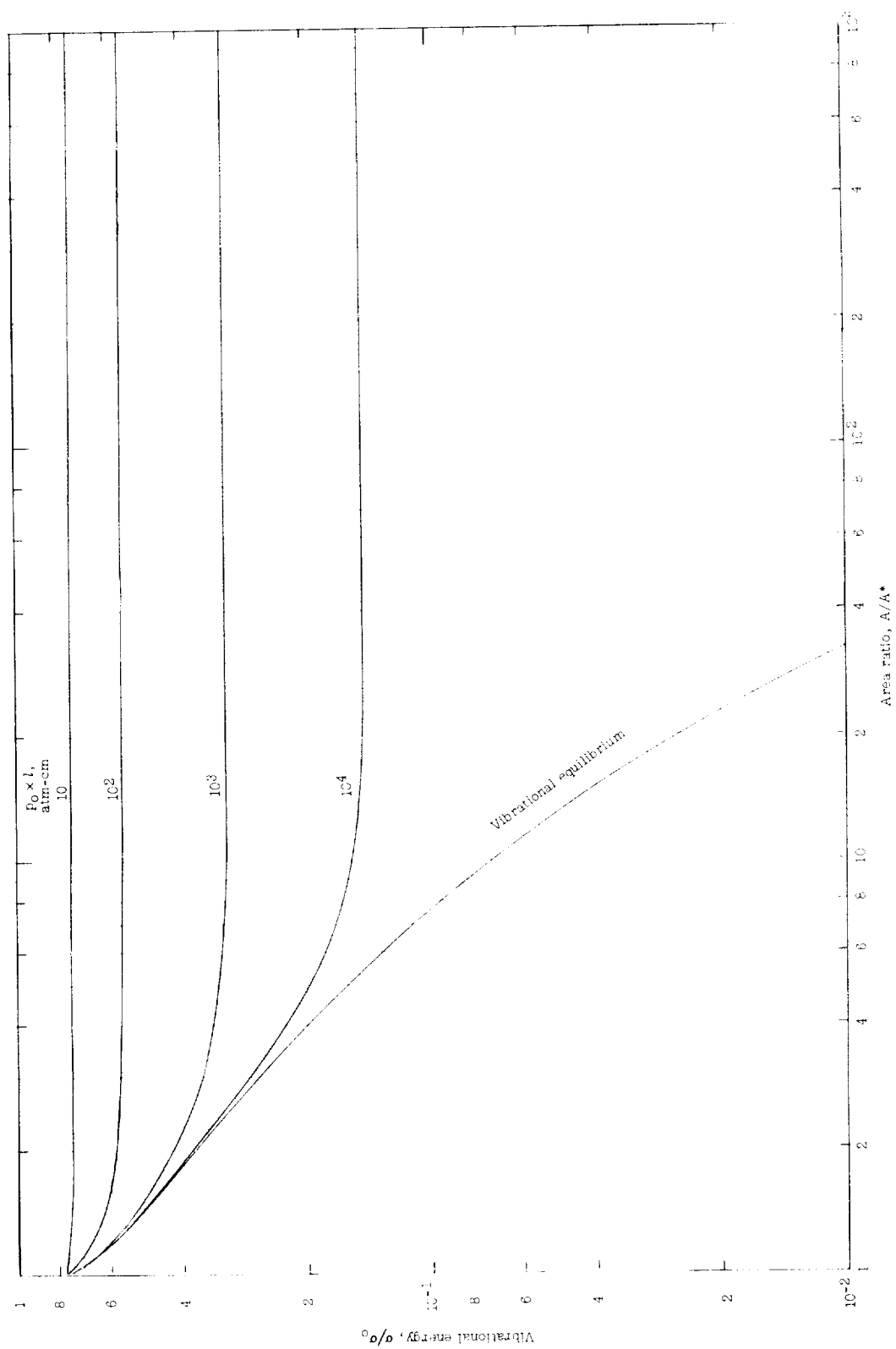


Figure 1.- Vibrational energy as function of area ratio for $T_0 = 3,000^\circ \text{K}$ and various values of parameter $P_0 \times l$.

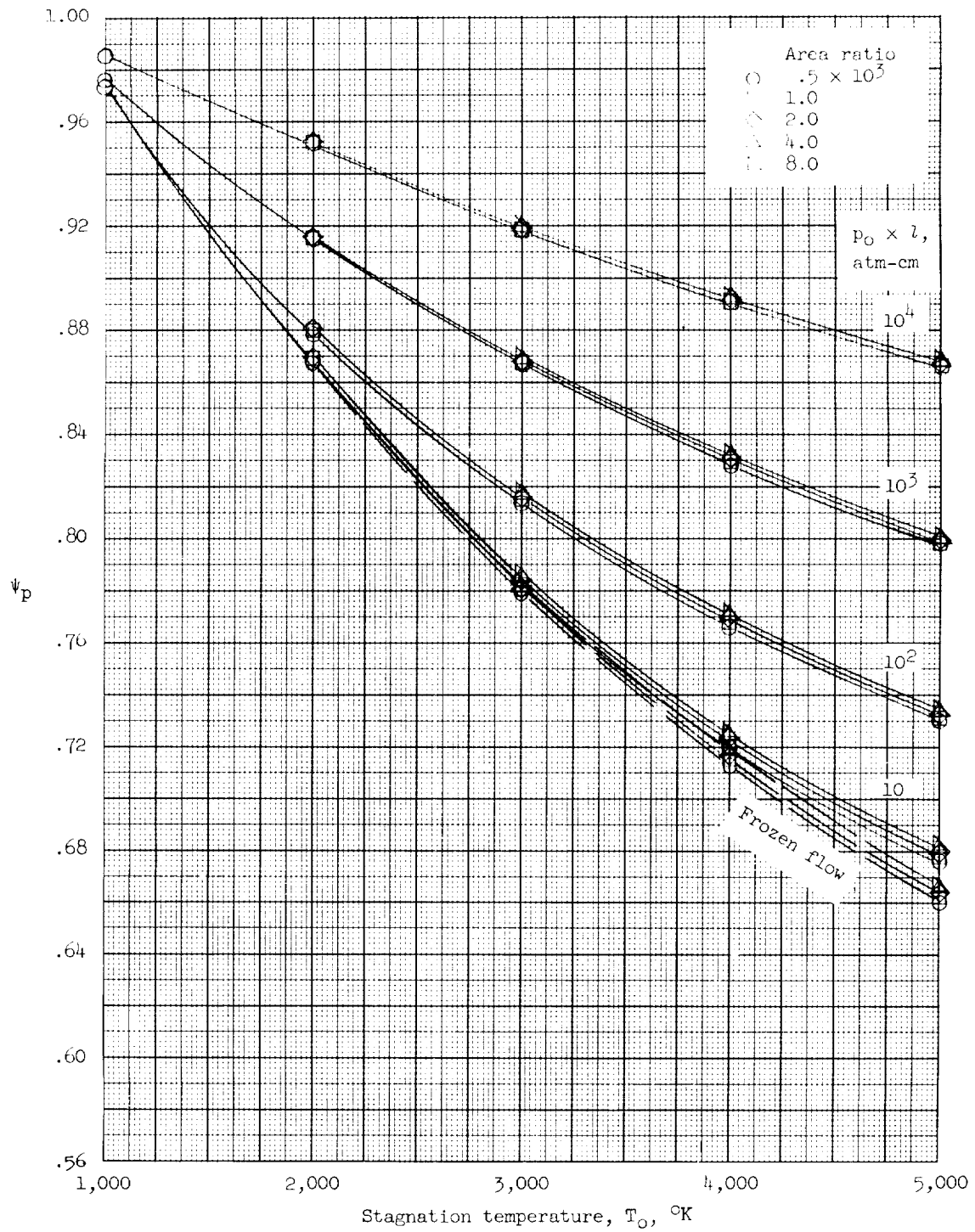


Figure 3.- Ratio of free-stream pressure based on vibrationally relaxing flow to that for equilibrium flow plotted against stagnation temperature for various combinations of area ratio and nozzle characteristic $p_o \times l$.

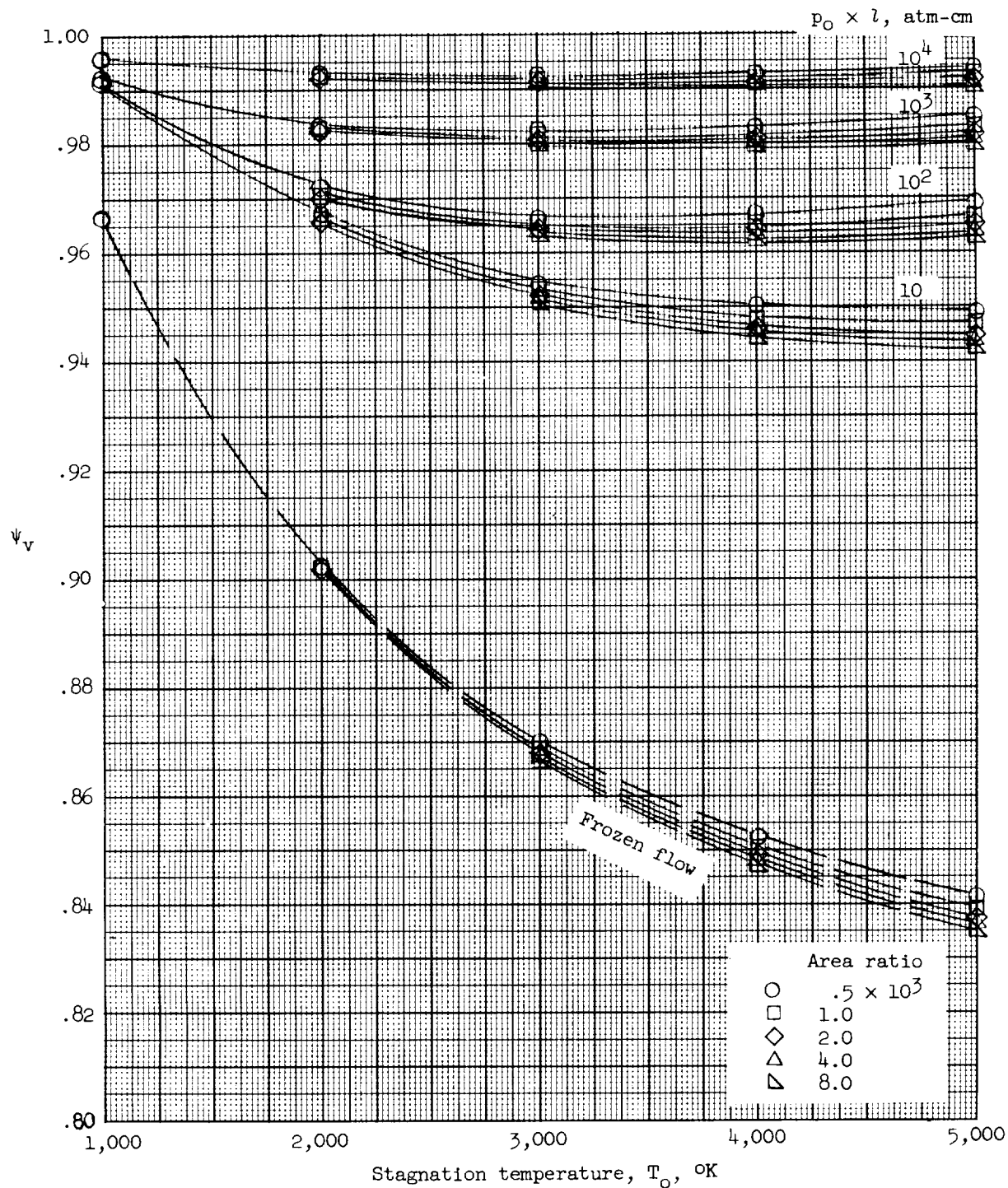


Figure 5.- Ratio of free-stream velocity based on vibrationally relaxing flow to that for equilibrium flow plotted against stagnation temperature for various combinations of area ratio and nozzle characteristic $p_0 \times l$.

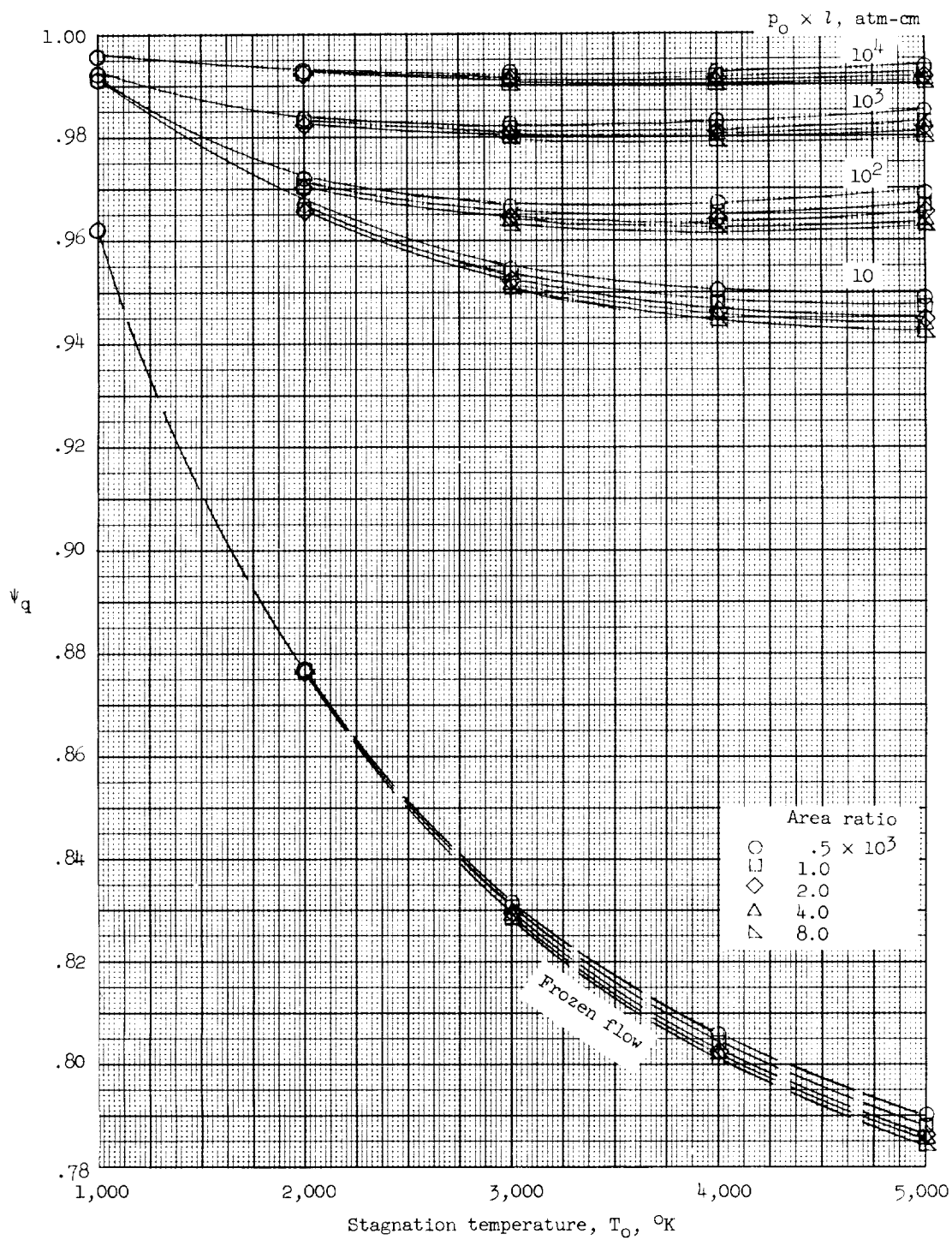


Figure 7.- Ratio of free-stream dynamic pressure based on vibrationally relaxing flow to that for equilibrium flow plotted against stagnation temperature for various combinations of area ratio and nozzle characteristic $p_0 \times l$.

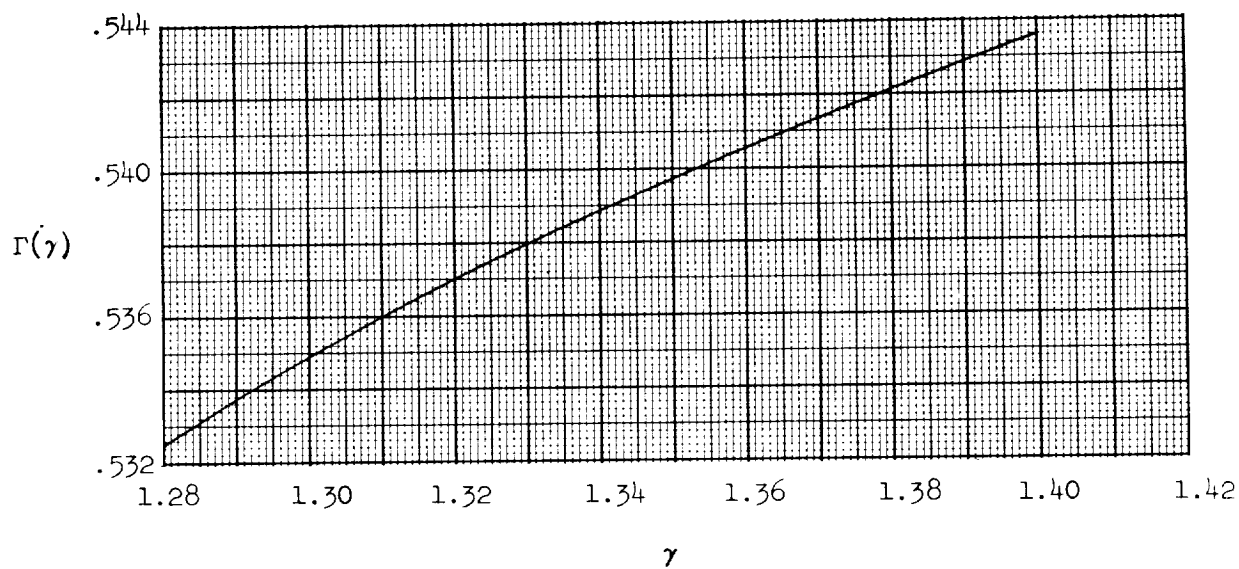


Figure 9.- $\Gamma(\gamma)$ plotted against γ .

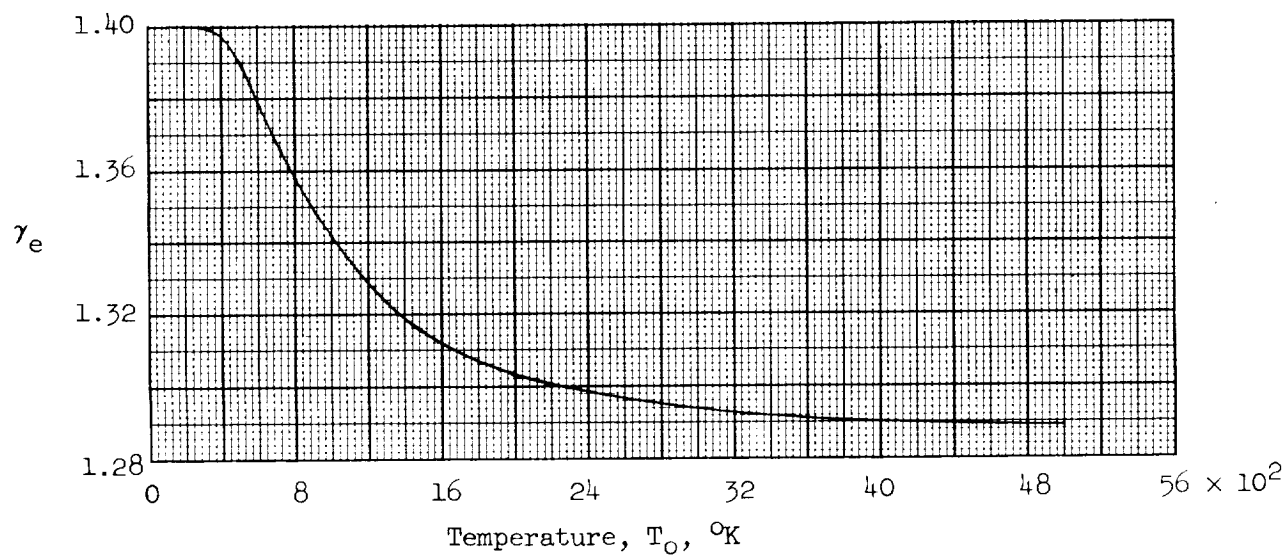


Figure 10.- Ratio of specific heats for vibrational equilibrium γ_e plotted against temperature.

ERRATA

NASA Technical Note D-1810

VIBRATIONAL-NONEQUILIBRIUM FLOW OF NITROGEN IN HYPERSONIC NOZZLES

By Wayne D. Erickson
June 1963

Page 6, line 20: The inequality $T_0 > 5,000^\circ \text{K}$ should be changed to read
 $T_0 < 5,000^\circ \text{K}$.

Page 13: Replace with revised page 13.

Page 14: Replace with revised page 14.

Page 15: Replace with revised page 15.

Page 23 (fig. 5): Replace with revised page 23 (fig. 5).

Page 25 (fig. 7): Replace with revised page 25 (fig. 7).

An additional comment should be helpful in regard to the revised version of figure 7. The curves for ψ_q for the frozen-flow case have been drawn separately in figure 7 in order that they may be read more easily, because they cross over the nonequilibrium curves for ψ_q at the lower values of $p_0 \times l$. It is not inconsistent that the nonequilibrium curves for the lower values of $p_0 \times l$ fall below the curves denoted as frozen flow. The curves marked frozen flow are based on a constant value of $\gamma = 7/5$ from the stagnation chamber to the test section of the nozzle and are included to facilitate the use of these charts by using the tabulated flow parameters presented in reference 8. However, the limiting case for the nonequilibrium calculations for the present method would be based on equilibrium flow up to the nozzle throat, followed by sudden freezing at the throat with a subsequent isentropic expansion at a constant value of $\gamma = 7/5$. Calculations made for this limiting case have shown that ψ_q can be less than $\psi_{q,f}$ for the frozen-flow case based on the same stagnation temperature, pressure, and area ratio. The values of ψ_q for all nonequilibrium cases calculated lie above the limiting curves for ψ_q .

Enclosures:

Pages 13, 14, 15, 23, 25

M is large, as is shown later. The flow ratio q/p_0 for this example is, therefore, 0.5394×10^{-3} .

With this value of q/p_0 and with the use of the tables presented in reference 8, which are based on a constant value of $\gamma = 7/5$, a rough estimate of the area ratio is found, namely, $A/A^* \approx 1,650$. For $T_0 = 3,000^\circ \text{K}$ and the quantity $p_0 \times l = 100 \text{ atm-cm}$, it is determined from figure 7 that $\psi_{q,f} = 0.959$ and $\psi_q = 0.965$. Because $\psi_{q,f}$ and ψ_q are weak functions of area ratio, only a very approximate value of A/A^* was required in order to use figure 7. The ratio of these two quantities $\psi_{q,f}/\psi_q$ represents the ratio of the parameter q based on the assumption of frozen flow with $\gamma = 7/5$ to that based on vibrational-nonequilibrium flow with $T_0 = 3,000^\circ \text{K}$, $p_0 \times l = 100 \text{ atm-cm}$, and $A/A^* \approx 1,650$. The exact value of A/A^* can now be determined by multiplying the ratio $\psi_{q,f}/\psi_q$ by the quantity q/p_0 to find the corresponding frozen-flow value of q/p_0 based on $\gamma = 7/5$; that is,

$$\left(\frac{q}{p_0}\right)_f = \frac{0.959}{0.965} (0.539 \times 10^{-3}) = 0.536 \times 10^{-3}$$

Again from the tabulated flow parameters for $\gamma = 7/5$ presented in reference 8, the value of A/A^* , that corresponds to $(q/p_0)_f = 0.536 \times 10^{-3}$, is equal to 1,664. This is the value for the area ratio for the nonequilibrium-flow case as well as for the frozen-flow case with $\gamma = 7/5$.

The corresponding values of the other free-stream parameters for frozen flow with $\gamma = 7/5$, also determined from reference 8, are:

$$\left(\frac{T}{T_0}\right)_f = 0.3016 \times 10^{-1}$$

$$\left(\frac{p}{p_0}\right)_f = 0.4764 \times 10^{-5}$$

$$\left(\frac{\rho}{\rho_0}\right)_f = 0.1580 \times 10^{-3}$$

$$\left(\frac{v}{a^*}\right)_f = 2.412269$$

$$M_f = 12.68$$

Because a^* is not the same for nonequilibrium flow as it is for frozen flow, it is not convenient to use the quantity $(v/a^*)_f$, but rather $(v/v_l)_f$. It is easily shown that for a flow with γ constant,

$$\left(\frac{a^*}{v_l}\right)_f = \sqrt{\frac{\gamma - 1}{\gamma + 1}} \quad (26)$$

so that for $\gamma = 7/5$, $\left(\frac{a^*}{v_l}\right)_f = \sqrt{\frac{1}{6}}$. For the present example then,

$$\left(\frac{v}{v_l}\right)_f = \left(\frac{v}{a^*}\right)_f \left(\frac{a^*}{v_l}\right)_f = 2.412269 \times \sqrt{\frac{1}{6}} = 0.985$$

From figures 2 to 6 for $T_0 = 3,000^\circ \text{K}$, $p_0 \times l = 100 \text{ atm-cm}$, and $A/A^* = 1,664$, the following ratios are determined:

$$\psi_{T,f} = 0.714; \psi_T = 0.788$$

$$\psi_{p,f} = 0.782; \psi_p = 0.815$$

$$\psi_{\rho,f} = 1.101; \psi_\rho = 1.036$$

$$\psi_{v,f} = 0.934; \psi_v = 0.965$$

and

$$\psi_{M,f} = 1.106; \psi_M = 1.088$$

It is now possible to determine the various free-stream parameters in the nozzle for nonequilibrium flow in addition to q/p_0 which has already been determined as 0.539×10^{-3} for this supposed case. For example, the nonequilibrium value of T/T_0 is calculated by multiplying $\psi_T/\psi_{T,f}$ by $(T/T_0)_f$. The other parameters, with the exception of v/v_l , are determined likewise, so that for this example the following numerical values are obtained:

$$\frac{T}{T_0} = \frac{\psi_T}{\psi_{T,f}} \left(\frac{T}{T_0}\right)_f = \frac{0.788}{0.714} (0.3016 \times 10^{-1}) = 0.333 \times 10^{-1}$$

$$\frac{p}{p_0} = \frac{\psi_p}{\psi_{p,f}} \left(\frac{p}{p_0}\right)_f = \frac{0.815}{0.782} (0.4764 \times 10^{-5}) = 0.497 \times 10^{-5}$$

$$\frac{\rho}{\rho_0} = \frac{\psi_\rho}{\psi_{\rho,f}} \left(\frac{\rho}{\rho_0}\right)_f = \frac{1.036}{1.101} (0.1580 \times 10^{-3}) = 0.1486 \times 10^{-3}$$

$$M = \frac{\psi_M}{\psi_{M,f}} M_f = \frac{1.088}{1.106} 12.68 = 12.49$$

Because the value of the limiting velocity v_l in the ratio $(v/v_l)_f$ differs from that calculated for the case with vibrational equilibrium in the stagnation chamber, the ratio v/v_l for the nonequilibrium case is determined in a similar way, but by multiplying by an additional term $v_l'/v_{l,e}$, which represents the ratio of the limiting velocity based on the exclusion of the vibrational energy term from the stagnation enthalpy to that based on a stagnation enthalpy for vibrational equilibrium. This term is presented in figure 11 as a function of T_0 and was calculated from the equation

$$\frac{v_l'}{v_{l,e}} = \sqrt{\frac{c_p' T_0}{c_p' T_0 + \sigma_{e,o}}} \quad (27)$$

The limiting-velocity ratio for this example is

$$\frac{v}{v_l} = \frac{\psi_v}{\psi_{v,f}} \left(\frac{v}{v_l} \right)_f \frac{v_l'}{v_{l,e}} = \frac{0.965}{0.934} (0.985)(0.930) = 0.947$$

where $v_l'/v_{l,e}$ is obtained from figure 11 for $T_0 = 3,000^\circ \text{K}$. These are the free-stream flow parameters based on nonequilibrium calculations for this illustrative example.

The charts presented herein may also be used to determine the flow parameters for vibrational-equilibrium flow. This may be done by using the foregoing method, but by setting ψ_q , ψ_T , ψ_p , ψ_ρ , ψ_v , and ψ_M equal to unity. These results, however, do not take into account the real-gas effect due to high densities.

Similar charts have been presented in the work of reference 9 for air for equilibrium flow that do include the real-gas effect due to high densities as well as vibrational energy. In order to obtain an approximate indication of this density effect in nitrogen, one may use the results of reference 9 for air to relate the real-gas equilibrium-flow parameters to those for frozen flow with $\gamma = 7/5$. The various ratios of the flow parameters presented in reference 9, as well as the correction factors presented in reference 8 for vibrational-equilibrium flow of air as an ideal gas, are presented as ratios at fixed Mach numbers rather than at fixed area ratios as in this work. The use of the ratios presented in references 8 and 9 is similar to the procedure presented herein, except it must be remembered that the ratios of the flow parameters for the present work are for the same area ratio.

The real-gas effect due to high densities could be included in the nonequilibrium-flow calculations by using values of $\psi_{q,f}$, $\psi_{T,f}$, $\psi_{p,f}$, $\psi_{\rho,f}$,

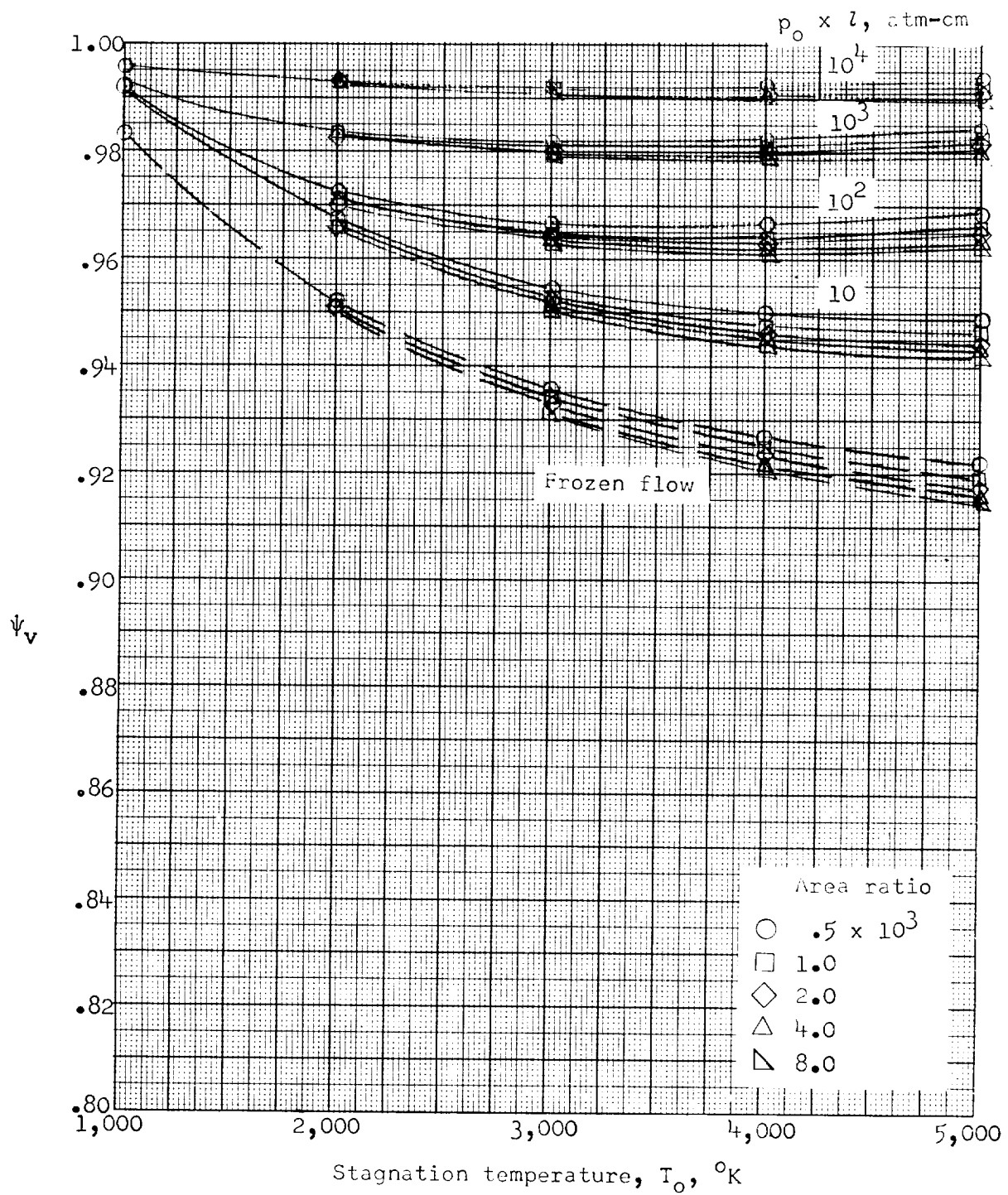


Figure 5.- Ratio of free-stream velocity based on vibrationally relaxing flow to that for equilibrium flow plotted against stagnation temperature for various combinations of area ratio and nozzle characteristic $p_0 \times l$.

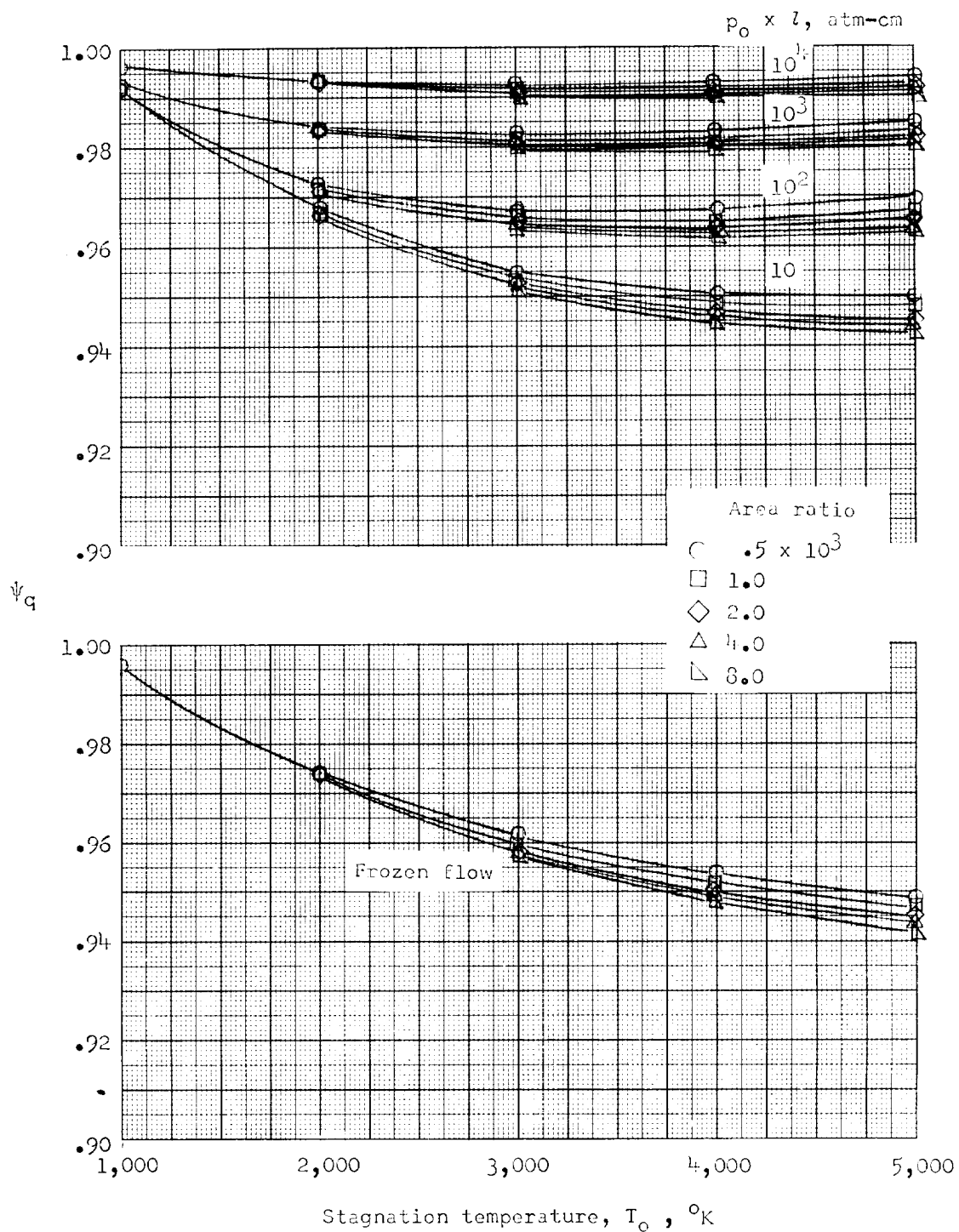


Figure 7.- Ratio of free-stream dynamic pressure based on vibrationally relaxing flow to that for equilibrium flow plotted against stagnation temperature for various combinations of area ratio and nozzle characteristic $p_0 \times l$.